# Analysis of current fluctuations in silicon $pn^+$ and $p^+n$ homojunctions

M. J. Martín, J. E. Velázquez, and D. Pardo
*Departamento de Física Aplicada, Facultad de Ciencias, Universidad de Salamanca, 37008 Salamanca, Spain*

(Received 28 November 1995; accepted for publication 31 January 1996)

A detailed study of bipolar transport under forward-bias conditions is evaluated by Ensemble Monte Carlo simulation in two structures ($p^+n$ and $pn^+$ junctions). The static characteristics of both structures are presented. In particular, this study focuses on a microscopic analysis of current fluctuations. A decomposition of the autocorrelation function of the total current fluctuations in electron, hole and crossed contributions is performed. In this way, the importance of each type of carrier in the spectral density of current fluctuations in both structures for a wide frequency range is determined. In the low frequency range, the presence of shot, thermal and excess noise was found. The Ensemble Monte Carlo method also permits ready evaluation of the noise equivalent temperature in both structures. © *1996 American Institute of Physics.* [S0021-8979(96)09409-7]

## I. INTRODUCTION

In the last fifteen years the development of technology for the manufacture of submicron devices has allowed the extension of the maximum frequency of oscillation ($f_{\max}$) into the millimeter-wave region (30–300 GHz). The optimal noise figure of devices working in this frequency region is an increasing function of frequency [for example, see the Fukui model for microwave metal–semiconductor field-effect transistor (MESFET)].[1] This means that, in practice, the useful amplification band (frequencies in which the signal-to-noise ratio is greater that one) was lower than $f_{\max}$. Hence, to design new high speed and low noise electronic devices it is essential to have available an adequate modelling of noise phenomena at high frequency. Accordingly, a good modelling of these phenomena begins with knowledge of the fluctuations in the microscopic processes of transport that cause noise (both in low and high frequencies).

The Ensemble Monte Carlo (EMC) method is the one most frequently used to study charge transport on submicron devices due to its ability to provide accurate results when carrier transport occurs under nonequilibrium carrier-lattice conditions.[2] This method not only provides meaningful physical quantities to describe the static and dynamic behavior of the device (mean velocity, current, carrier density, etc.) but also affords its fluctuations. An essential characteristic of the EMC is that it allows one to gain a microscopic understanding of the different noise sources because these are included in the simulations without introducing additional assumptions into the microscopic transport model.[3]

Quite recently the development of high frequency devices (larger than 10 GHz) has focused on unipolar technologies. However, the recent development of bipolar technology, such as that based on a Si-Ge[4,5] alloy, has allowed the manufacture of high-performance heterojunction bipolar transistors (HBTs). This has emphasized the importance of a detailed characterization of noise performances in bipolar devices. The study of this can be carried out by means of the EMC method, which has been successfully employed to investigate the fluctuations in different high speed unipolar devices: $n^+nn^+$ junctions, Schottky diodes and GaAs MESFET.[6–9]

Study of the noise phenomena occurring in a heterojunction is a complex problem because many physical mechanisms responsible for different noise sources (lattice phonons and charged impurity scattering, fluctuations in barrier height, quantum transport at heterojunction, energy levels quantization, carrier mass change between both sides of the union, etc.) are involved. For such purposes, a first step involves studying bipolar homojunctions in order to clearly determine the origin of the current fluctuations due to the classic transport, which is of diffusive type. In this article we report a MC analysis of noise in basic bipolar structures (Si $p^+n$ and $pn^+$ homojunctions) and perform a physical interpretation of the total current fluctuations in terms of the electron, hole and crossed (electron-hole and hole-electron) contributions.

The article is organized as follows: In Section II, the details of the simulated structures, the Si physical model and the characteristics of the EMC method together with the parameters used in the simulation are described. In Section III we offer a theoretical analysis of the calculated magnitudes together with the previously performed decomposition of the autocorrelation function and of the spectral density of total current in terms of the electron, hole and crossed contributions. Section IV offers the simulation results, the static characteristics—which is the first and important step in the study of fluctuations—and the study of current noise for both structures. Finally, in Section V we offer the main conclusions.

## II. DEVICE MODEL SIMULATOR: UNIDIMENSIONAL ENSEMBLE MONTE CARLO

The simulated structures are modelled as abrupt Si $pn^+$ and $p^+n$ junctions. We assume the absence of bidimensional effects in the devices and the study is carried out in the [100] crystallographic direction. The doping level of the $n^+$ and $p^+$ regions is $10^{17}$ cm$^{-3}$ and such regions are 0.3 $\mu$m long whereas the $n$ and $p$ regions of doping density is $5\times10^{15}$ cm$^{-3}$ and these regions are 0.4 $\mu$m long. According to these doping densities, the built-in potential ($V_{\rm bi}$) is 0.735 V (300 K). Ohmic contacts were placed at both ends of the structures where the carriers are injected into the device, up-

TABLE I. Parameters for Si holes used in the simulation.

| Parameter | | | Unit |
|---|---|---|---|
| Acoustic deformation potential[a] | 5.0 | | eV |
| Optical deformation potential[a] | $26.6\times10^{10}$ | | eV/m |
| Acoustic phonon energy[b] | 1.05 | | meV |
| Optical phonon temperature[b] | 735 | | K |
| | Heavy band | Light band | |
| Effective mass[c] | $0.537\ m_0$ | $0.153\ m_0$ | |
| Non-parabolicity | 0.9 | 0.6 | $eV^{-1}$ |

[a]See Ref. 13.
[b]See Ref. 14.
[c]See Ref. 12.

dating the number of electrons and holes considered. These contacts are characterized because the neutrality is maintained in a region close to the contact by injecting at each time step the number of thermal electrons necessary to equal the free-carrier concentration to the impurity density. In addition, any carrier reaching the contact leaves the device. To account for the higher probability of particles with a large velocity to enter the device, the velocity of the particles is chosen randomly according to a Maxwellian distribution function weighted by the velocity component perpendicular to the contact and directed into the device.[10]

The microscopic model implemented in the simulator enables one to follow the electron and hole dynamics simultaneously. The band structure considered includes the $X$ and the $L$ valleys of the conduction band anisotropically.[11] The valence band model includes two nonparabolic bands (heavy and light) degenerated at the $\Gamma$ point with spherical energy surfaces. The Si hole parameters used in the simulation are shown in Table I. Owing to the particular form of the valence band, intraband as well as interband transitions must be taken into account in each type of scattering mechanism. Here, we consider inelastic acoustic, nonpolar optic scattering and ionized impurity interactions. The overlap expressions for intra- and interband transitions are included when selecting the final state after scattering. As has been discussed previously,[14–16] acoustic phonon scattering must be considered as an inelastic process. The small exchange of energy between charge carriers and the lattice in a single scattering event is necessary to achieve available stationary conditions at low electric fields and low temperatures. With the inclusion of these models, the drift velocity-electric field characteristics obtained for bulk Si show excellent agreement with the experimental results both for electrons and for holes.[15–17]

Calculation of the physical quantities of interest is carried out following the standard scheme;[2] that is, by self-consistently coupling the EMC simulator (three-dimensional in $k$-space and one-dimensional in real space) with a Poisson solver algorithm that allows one to obtain the spatial distribution of electric potential. Generation-recombination phenomena (band-band, band-impurities, ...) were not considered due to the small length of the devices.

To reduce the large CPU time necessary in very low forward bias conditions, in which the minority carrier density is very small, a real-space repetition scheme[18] was implemented. This scheme allows us to maintain a quasiconstant number of simulated particles in all cells instead of the large concentration gradients that appear in the devices. The device is divided into equal cells of 100 Å each; these are sufficiently small to reproduce the spatial variations in the electric potential. The time step, $DT$, to solve the Poisson equation is 10 fs. The mean number of simulated particles changes with bias. As an example, in the $p^+n$ structure for a voltage of 0.8 V this number is about 10500.

## III. THEORETICAL ANALYSIS

To analyze the current fluctuations in the current-noise operation mode the voltage applied to the electrodes must remain constant.[3] Under these conditions the displacement current between electrodes is null. In a one-dimensional bipolar structure of length $L$, the conduction current, $I(t)$, is given by:

$$I(t)=\frac{q}{L}\sum_{i=1}^{N_{Te}(t)} v_i(t)-\frac{q}{L}\sum_{j=1}^{N_{Th}(t)} v_j(t) \tag{1}$$

where $q$ is the absolute value of the electron charge, $v_i(t)$ and $v_j(t)$ are the instantaneous velocities along the electric field direction of the $i$th electron or the $j$th hole, and $N_{\mathrm{te}}(t)$ and $N_{\mathrm{th}}(t)$ are the total number of electrons or holes, respectively, inside the device.

In order to obtain the total current fluctuations in terms of the contributions of electrons and holes, $I(t)$ can also be expressed as:

$$I(t)=I_e(t)+I_h(t), \tag{2}$$

where $I_e(t)$ is the electron current and $I_h(t)$ the hole current.

The mathematical quantity that characterizes the current noise is the autocorrelation function of the total current fluctuations $C_I(t)$, given by

$$C_I(t)=\overline{\delta I(0)\,\delta I(t)}, \tag{3}$$

where $\delta I(t)=I(t)-\overline{I}$ are the total current fluctuations (where the upper bar indicates time average).

Then the autocorrelation function of the total current fluctuations is therefore given by:

$$C_I(t)=C_{Ie}+C_{Ih}+C_{Ic}, \tag{4}$$

where:

$$C_{Ie}=\overline{\delta I_e(0)\,\delta I_e(t)}, \tag{5}$$

$$C_{Ih}=\overline{\delta I_h(0)\,\delta I_h(t)}, \tag{6}$$

$$C_{Ic}=\overline{\delta I_e(0)\,\delta I_h(t)}+\overline{\delta I_h(0)\,\delta I_e(t)} \tag{7}$$

are the terms associated with different contributions to the total current autocorrelation function. $C_{Ie}$ is associated with the electron current fluctuation, $C_{Ih}$ is associated with the hole current fluctuation, and $C_{Ic}$ is associated with the cross correlation between electron and hole current fluctuations.

According to the Wiener-Kintchine theorem,[19] the spectral density of current fluctuations is obtained from the autocorrelation functions as its Fourier transform:

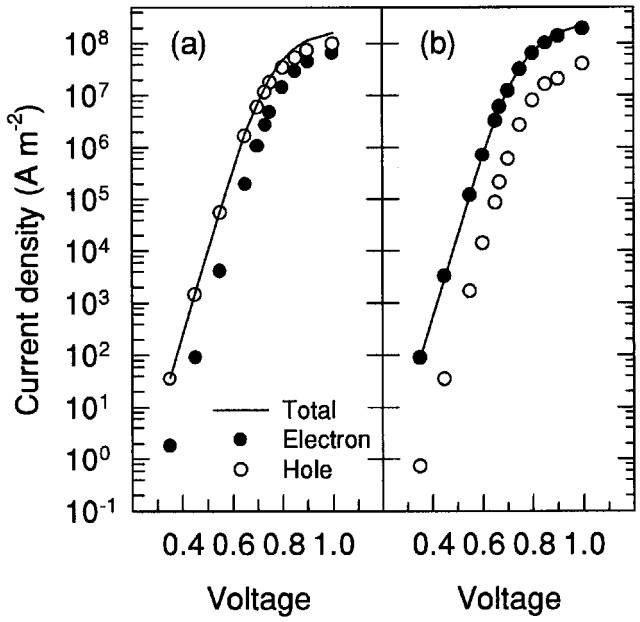


FIG. 1. Total current density (continuous line), electron current (closed symbols) and hole current (open symbols) as a function of applied bias: (a) for the $p^+n$ structure and (b) for the $pn^+$ structure.

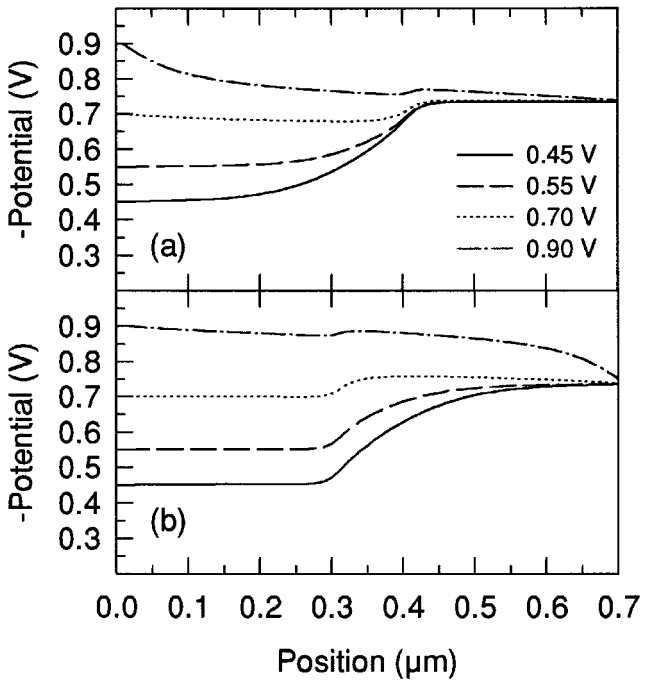


FIG. 2. Profiles of potential as a function of the position in the (a) $pn^+$ and (b) $p^+n$ structures for different forward biases.

$$S_I(f)=2\int_{-\infty}^{\infty} C_I(t)e^{j2\pi ft}\,dt=S_{Ie}+S_{Ih}+S_{Ic}, \tag{8}$$

where:

$$S_{Ie}(f)=2\int_{-\infty}^{\infty} C_{Ie}(t)e^{j2\pi ft}\,dt, \tag{9}$$

$$S_{Ih}(f)=2\int_{-\infty}^{\infty} C_{Ih}(t)e^{j2\pi ft}\,dt, \tag{10}$$

$$S_{Ic}(f)=2\int_{-\infty}^{\infty} C_{Ic}(t)e^{j2\pi ft}\,dt. \tag{11}$$

Once the stationary situation has been reached, at each time step the $I_e(t)$ and $I_h(t)$ values are recorded to calculate the autocorrelation and cross-correlation functions. Under stationary conditions, in the $p^+n$ structure for the applied voltage of 0.8 V, the deviation in the number of simulated particles—around the mean value—is about 5%. Owing to the characteristics of the bipolar device transport it was necessary to perform the simulation over 1 ns after a transient period of 20 ps to obtain a suitable convergence of the autocorrelation and cross-correlation functions.

## IV. RESULTS

### A. Static characteristics

Before reporting the results of noise analysis, we offer the main static results. Figure 1 shows the total forward current-voltage characteristics of the (a) $p^+n$ and (b) $pn^+$ structures. The electron and hole currents are also plotted. Figure 2 shows the potential profile of the structures for different forward bias ($V_{\text{appl}}$). It may be seen from this figure that when $V_{\text{appl}}<V_{\text{bi}}$ the whole of the potential drop is essentially localized in the spatial charge region of the junctions (barrier-limited current transport) and almost all the spatial charge region is located in the low doping region, in agreement with the classic results of the Schockley model. In this bias range (300 mV$<V_{\text{appl}}<$600 mV), the simulation results show that the current in both structures follows exponential behavior, in agreement with the theoretical equation of a short diode.[20] In both structures, for applied voltages above $V_{\text{bi}}$ the junction barrier disappears and the voltage drops along the whole device. Under these conditions the junctions behave as a ''resistance'' varying with the bias.

In the range of barrier-limited current, Figure 1, the total current is essentially due to the majority carriers of the highly doped region (electrons in the $pn^+$ junction and holes in the $p^+n$ one). Nevertheless, for $V_{\text{appl}}>V_{\text{bi}}$, in the $pn^+$ diode the total current is still mainly due to the electron current whereas in the $p^+n$ diode the high mobility of the electrons means that their contribution to the total current becomes comparable to the hole current. Below we show that this elicits a different kind of noise behavior between both structures.

### B. Noise results

In this section we present the results obtained concerning the autocorrelation functions and the spectral density of current fluctuations, as well as the different terms into which these have been divided.

Figures 3(a) and (b) show the results of the autocorrelation function of the total current fluctuations ($C_I$) for different forward voltages applied, respectively, to the $pn^+$ and $p^+n$ diodes. In general $C_I$ exhibits a negative part which decreases with the forward bias. However, $C_I$ is modified in each structure in different ways when bias increases. The differences in $C_I$ between both structures can be analyzed in

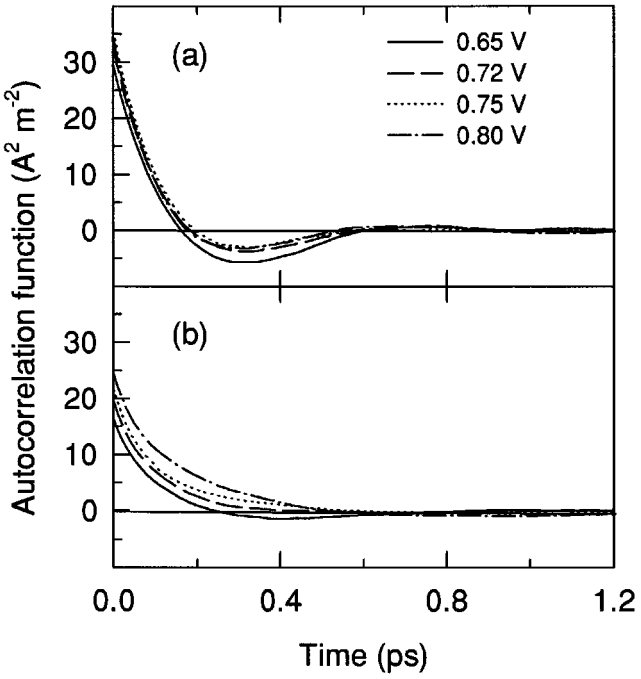


FIG. 3. Autocorrelation function of total current fluctuations as a function of time of the (a) $pn^+$ and (b) $p^+n$ structures for different applied voltages.

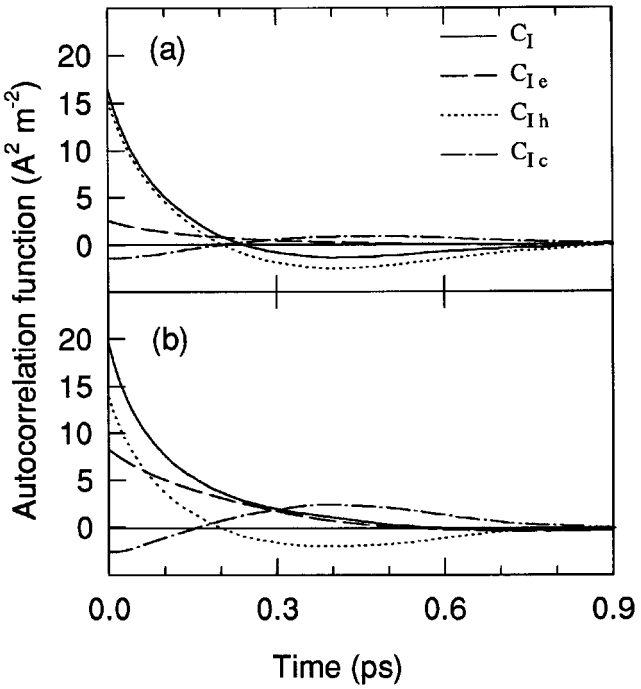


FIG. 5. Decomposition of the autocorrelation function of total current fluctuations in the $p^+n$ structure for 0.65 V (a) and 0.75 V (b) forward bias.

terms of its components: autocorrelation functions of electron current fluctuations, $C_{Ie}$, hole current fluctuations, $C_{Ih}$, and cross-correlation functions of current fluctuations, $C_{Ic}$.

Figure 4 shows the $C_I$ decomposition for the $pn^+$ structure for the applied voltages (a) 0.65 V and (b) 0.75 V. Figure 5 shows a similar decomposition for the $p^+n$ structure where the calculations are performed under the same voltage conditions. It may be seen in both structures and for all biases that $C_{Ie}$ and $C_{Ih}$ are characterized by an exponential decay (associated with the momentum relaxation due to scattering processes) and a negative part commonly attributed to the coupling between the fluctuations of the electric field and the carrier velocity fluctuations. This coupling requires the presence of an inhomogeneity in the structure.[7]

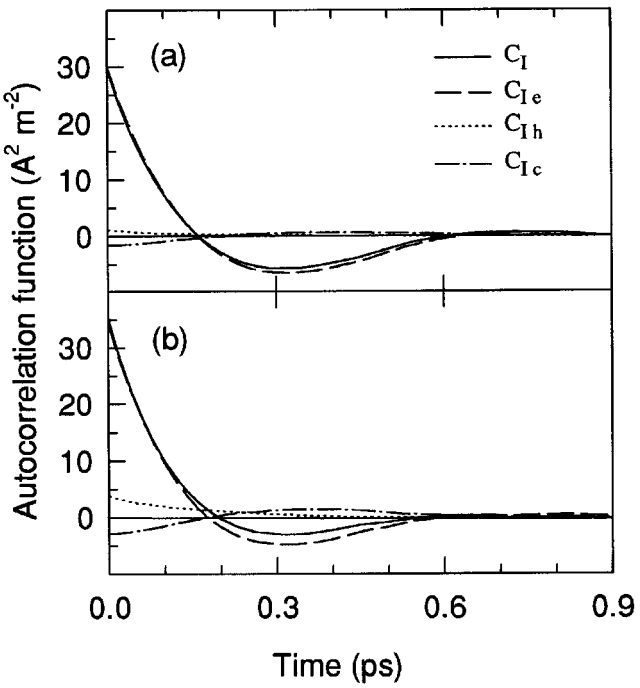


FIG. 4. Decomposition of the autocorrelation function of total current fluctuations in the $pn^+$ structure for (a) 0.65 V and (b) 0.75 V forward bias.

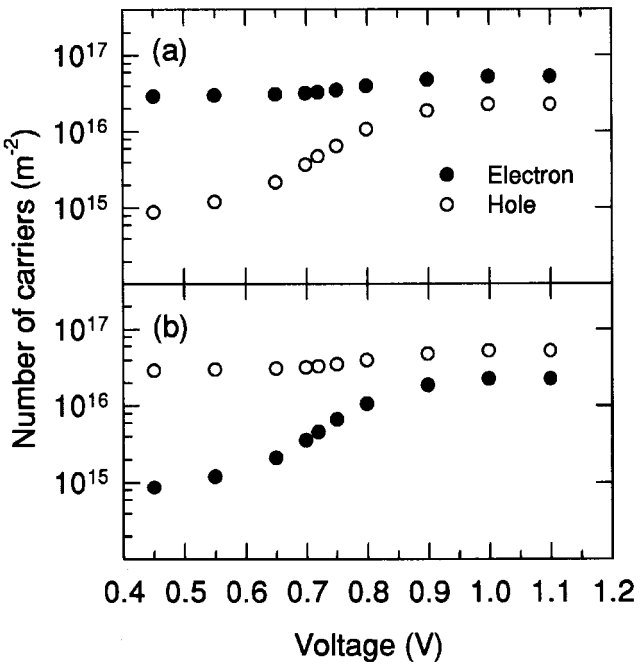


FIG. 6. Carrier number inside the (a) $pn^+$ and (b) $p^+n$ structures as a function of forward bias. Open and closed symbols correspond to electrons and holes number, respectively.

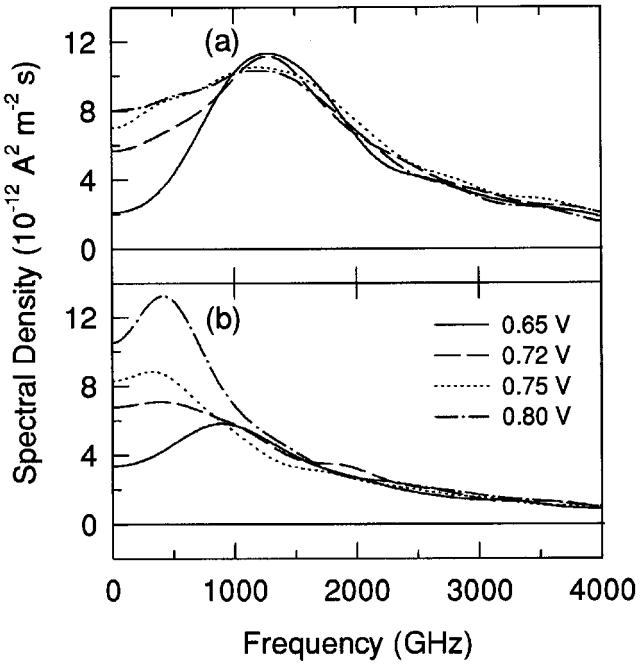


FIG. 7. Spectral density of total current fluctuations of (a) $pn^+$ and (b) $p^+n$ structures as a function of frequency for different applied voltages.

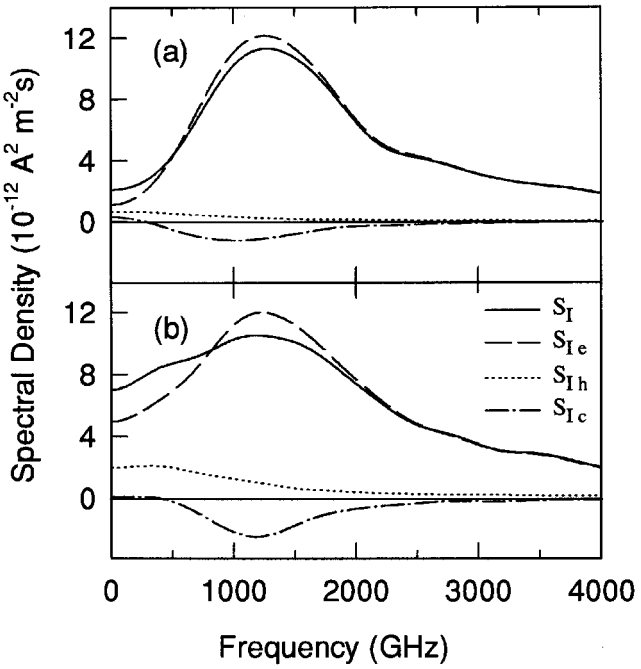


FIG. 8. Decomposition of the spectral density of total current fluctuations in the $pn^+$ structure for (a) 0.65 V and (b) 0.75 V forward bias.

Taking into account that current fluctuations can be originated by fluctuations in velocity and carrier numbers (present inside the structure) and in order to analyze the role played by each of these terms, $C_{Ie}$, $C_{Ih}$ and $C_{Ic}$ have been subdivided into terms associated with the autocorrelation functions of carrier velocity and carrier number fluctuations.[21] The highly doped regions of the structures ($n^+$ or $p^+$ means that the autocorrelation function of carrier number fluctuations is negligible in comparison with the autocorrelation function of velocity fluctuations (at least at four orders of magnitude), as confirmed in the simulation. The presence of strong space-charge effects tends to suppress the number fluctuations through the long range Coulomb interaction.[7] Thus, $C_{Ie}$, $C_{Ih}$ and $C_{Ic}$ are only determined by the contribution of the autocorrelation function of velocity fluctuations. This contribution is expressed in terms of the mean number of particles and the velocity fluctuations.[3] This implies that the increase in $C_{Ie}$, $C_{Ih}$ due to the increase in bias would be due to the increase in both the mean carrier number and the carrier velocity fluctuations. In Figure 6, which shows the dependence on voltage of the mean number of electrons and holes present inside the device per square meter, it may be seen that the increase in the mean number of the majority and the minority carriers with voltage is similar in both structures. Accordingly, the difference between the autocorrelation functions of minority current fluctuations in both structures is only due to the velocity fluctuations. As a consequence, the increase in the autocorrelation function of minority current fluctuation with voltage is greater in the $p^+n$ structure (in accordance with the density current behavior), basically due to the greater mobility of the electrons.

In the $pn^+$ structure (Figure 4), regardless of the presence of the barrier, $C_I$ is essentially determined by the $C_{Ie}$ contribution (majority carriers of the highly doped region), although at very high bias the $C_{Ih}$ and $C_{Ic}$ contributions become significant. Figure 5 shows that in the $p^+n$ structure the $C_{Ie}$ and the $C_{Ic}$ contributions have an essential and increasing weight when forward bias increases. This means that in this structure $C_I$ does not display any clear kind of behavior determined for one type of carrier (holes) but rather that it is a combination of all contributions. This important increase in the electron contribution with bias was previously observed in the static current-voltage characteristic of the $p^+n$ structure.

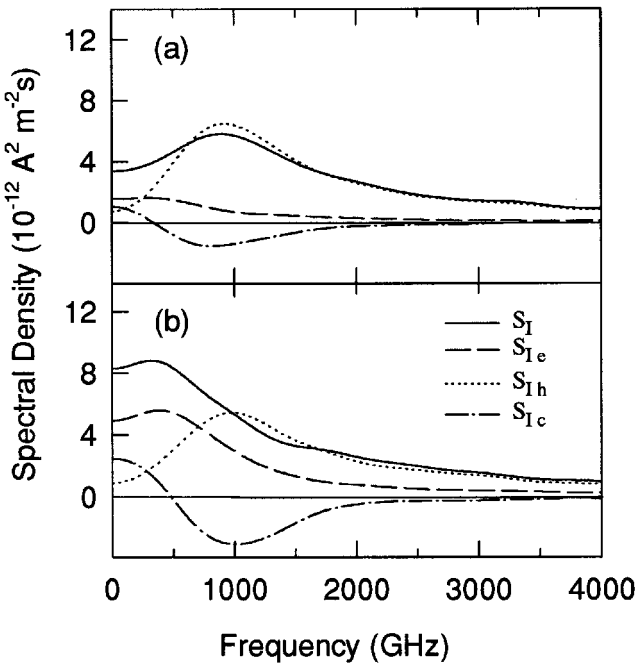


FIG. 9. Decomposition of the spectral density of total current fluctuations in the $p^+n$ structure for (a) 0.65 V and (b) 0.75 V forward bias.

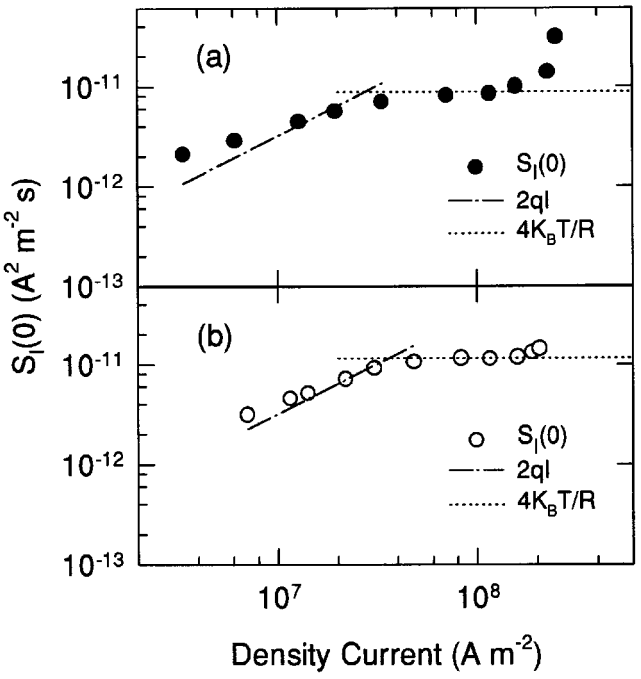


FIG. 10. Low-frequency value of the spectral density of current fluctuations as a function of the total current flowing through the (a) $pn^+$ and (b) $p^+n$ structures. Symbols refer to Monte Carlo calculations.

The spectral-density of total current fluctuations ($S_I$) is the quantity which describes the microscopic noise in different frequency ranges. The results of $S_I$ obtained by Fourier transforming the autocorrelation function of current fluctuations (Figure 3) are plotted in Figure 7. Note that for the $pn^+$ diode both the frequency of the spectral density maximum (around 1200 GHz) and its amplitude remain practically constant with bias. However, in the $p^+n$ structure both quantities are strongly modified when forward bias is increased.

To analyze these results, we turn to the decomposition of the spectral density of total current fluctuations. The corresponding results of the $pn^+$ structure are shown in Figure 8(a) for $V=0.65$ V and (b) for $V=0.75$ V. $S_{Ie}$ is the main contribution of the total spectral density in this structure.

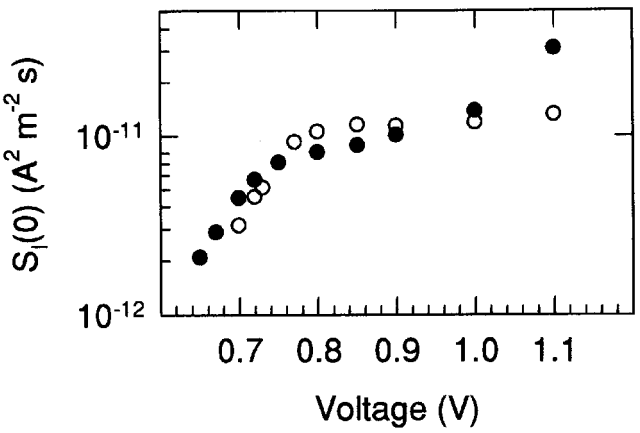


FIG. 11. Monte Carlo calculation of low-frequency value of the spectral density of current fluctuations as a function of bias in the $pn^+$ (closed symbols) and $p^+n$ (open symbols) structures.

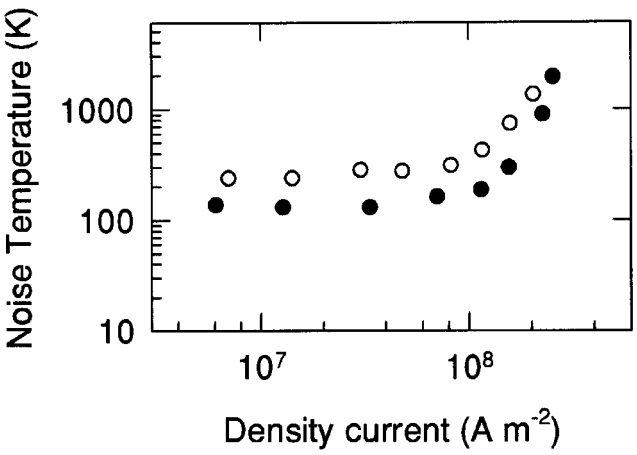


FIG. 12. Equivalent noise temperature at low frequency as a function of the total density current in the $pn^+$ (closed symbols) and $p^+n$ (open symbols) structures.

Accordingly, the frequency of the $S_I$ maximum (associated with the negative part of $C_I$) is related to the plasma frequency of the electrons in the $n^+$ region. The results of the $p^+n$ junction are plotted in Figure 9 and correspond to the same bias conditions used in Figure 8. When the barrier remains [Figure 9(a)] the influence of the minority carriers (electrons) is considerable at low frequencies but these have no effect on the spectral density maximum, which is only related to the plasma frequency of the holes in the $p^+$ region (around 1000 GHz). For high forward bias [Figure 9(b)], it can be seen that the $S_{Ie}$ and $S_{Ic}$ contributions lead to changes in the frequency of the total spectral density maximum. This maximum is now characterized by the plasma frequency of the electrons in the $n$ region (around 400 GHz). As pointed out earlier, the origin of this change lies in the effect of the electrons when the barrier disappears. Moreover, for $V_{\text{appl}} > 0.75$ V the increase in the number of carriers with high mobility in this structure (Figure 6) causes a slight increase in the frequency of the spectral density maximum (Figure 7).

The spectral density at low-frequency, $S_I(0)$, as a function of the forward current in the structures is shown in Figure 10. For both junctions, in the low current region ($V_{\text{appl}} < V_{\text{bi}}$) $S_I(0)$ exhibits a dependence close to $2qI_T$, where $I_T$ is the total current. This behavior is typical of a shot noise region caused by the carrier crossing the barrier individually and at random.[22] In the intermediate current region, the noise is attributed to the fluctuations of the carrier velocity (thermal noise). In this region, $S_I(0)$ tends towards a value close to $4K_BT/R$, where $K_B$ is the Boltzmann constant, $T$ the lattice temperature and $R$ the ''differential'' resistance of the junctions when $V_{\text{appl}} \approx V_{\text{bi}}$. At the highest current, the presence of hot carriers is responsible for excess noise, leading $S_I(0)$ to increase considerably.

Figure 11 shows the spectral density at low frequencies of both structures as a function of forward bias. For low bias, $S_I(0)$ takes lower values in the $p^+n$ structure, corresponding to a lower current level. However, when bias increases the low frequency spectral density tends to saturation value (like the current density behavior) that is greater in the $p^+n$ structure. Moreover, for very high voltages an important increase in $S_I(0)$ only appears in the $pn^+$ diode. The differences be-

tween both structures at these voltages can be explained in terms of the presence of hot carriers. When there is no barrier, most of the voltage drop occurs in the low doping region (Figure 2). The voltage drop is responsible for the high values of the electric field in that region. The simulation results show that in the $p$ region of the $pn^+$ diode the electrons reach a mean energy maximum of 0.14 eV for the extreme applied voltage of 1.1 V, whereas in the $p^+n$ structure the mean energy of holes only reaches 0.075 eV in the $n$ region under the same bias conditions. This electron heating explains the different behavior of $S_I(0)$ between both structures at high applied voltages.

Finally, Figure 12 shows the noise equivalent temperature at low frequencies[6] as a function of the current density of both structures. It may be seen that the calculated noise equivalent temperature is greater in the $p^+n$ structure for all density current levels. This fact arises from the different dependence on the voltage of the admittance in both structures, in contrast to the $S_I(0)$ results (Figure 11). In the low current range, corresponding to the exponential region of the current-voltage characteristics, the noise temperature tends towards a value close to one half of the lattice temperature. This points to a full shot noise behavior.[22] As current increases, thermal noise becomes important and noise temperature increases towards the lattice temperature. For the highest currents, noise temperature surpasses the lattice temperature due to the hot carrier effect remarked above.

## V. CONCLUSIONS

Using self-consistent coupling of the EMC simulator (three-dimensional in $k$ space and one dimensional in real space) with a Poisson solver algorithm we have analyzed both the static characteristics and the current fluctuations in bipolar homojunctions: $p^+n$ and $pn^+$. The current-voltage static characteristics show exponential behavior when the barrier remains. For high forward bias (greater than the barrier height) the junctions exhibit ''resistor-like'' behavior. In this region, the different mobility of the majority carriers of both structures establishes an important difference in the noise results between both structures.

Through current fluctuations the spectral density of the total current is obtained for both structures. By decomposing the spectral densities in electron, hole and crossed contributions it is possible to evaluate the influence of the minority carriers (electrons in the $p^+n$ structure and holes in the $pn^+$ one) on the noise behavior of each structure. Whereas the holes in the $pn^+$ structure have no decisive influence, the electrons in the $p^+n$ structure have an important effect both on the current-voltage static characteristics and the noise results. As consequence, in this structure the electron contribution causes a decrease in the frequency of the spectral density maximum when voltage is increased. At low frequency, depending on the value of the current density, the presence of shot, thermal and excess noise can be observed. Excess noise due to the onset of hot carriers was found mainly in the $pn^+$ diode. The simulation results indicate that for all density current levels the noise equivalent temperature is greater in the $p^+n$ structure.

## ACKNOWLEDGMENTS

The authors wish to thank Dr. T. Gonzalez for his valuable discussions concerning the present subject. This work has been funded through the research Project No. TIC95-0652 from the CICYT.

[1] H. Fukui, IEEE Trans. Electron Devices **ED-26**, 1032 (1979).
[2] C. Jacoboni and P. Lugli, *The Monte Carlo Method for Semiconductor Device Simulation* (Springer, Vienna, 1989).
[3] L. Reggiani, T. Kuhn, and L. Varani, Appl. Phys. A **54**, 411 (1992).
[4] J. N. Burghartz, K. A. Jenkins, D. A. Grützmacher, T.O. Sedgwick, and C. L. Stanis, IEEE Electron Device Lett. **15,** 360 (1994).
[5] J. D. Cressler, E. F. Crabbé, J. H. Comfort, J. Y.-C. Sun, and J. M. Stork, IEEE Electron Device Lett. **15,** 472 (1994).
[6] J. Zimmermann and E. Constant, Solid-State Electron. **23**, 915 (1980).
[7] L. Varani, T. Kuhn, L. Reggiani, and Y. Perlès, Solid-State Electron. **36**, 251 (1993).
[8] T. González, D. Pardo, L. Varani, and L. Reggiani, Appl. Phys. Lett. **63**, 3040 (1993).
[9] T. González, D. Pardo, L. Varani, and L. Reggiani, IEEE Trans. Electron Devices **42,** 991 (1995).
[10] S. E. Laux and M. V. Fischetti, in *Monte Carlo Device Simulation: Full Band and Beyond*, edited by K. Hess (Kluwer, Boston, 1991).
[11] M. J. Martín, T. González, J. Velázquez, and D. Pardo, Semicond. Sci. Technol. **8**, 1291 (1993).
[12] O. Madelung, *Semiconductors: Group IV Elements and II-V Compounds* (Springer, Berlin, 1991).
[13] L. Reggiani, Proceedings of the 15th International Conference Physics of Semiconductors, edited by S. Tanaka and Y. Toyozawa, Kyoto, 1980 (unpublished), p. 467.
[14] S. Bosi, C. Jacoboni, and L. Reggiani, J. Phys. C Solid State Phys. **12**, 1525 (1979).
[15] C. Canali, F. Jacoboni, F. Nava, G. Ottaviani, and A. Alberigi-Quaranta, Phys. Rev. B **12**, 2265 (1975).
[16] T. Brudevol, T. A. Fjeldly, J. Baek, and S. Shur, J. Appl. Phys. **67**, 7373 (1990).
[17] G. Ottaviani, L. Reggiani, C. Canali, F. Nava, and A. Alberigi-Quaranta, Phys. Rev. B **12**, 3318 (1975).
[18] P. Lugli, in *Compound Semiconductor Device Modelling*, edited by C. M. Snowden and R. E. Miles (Springer, London, 1993).
[19] D. A. McQuarrier, *Statistical Mechanics* (Harper and Row, New York, 1976).
[20] S. Tiwari, *Compound Semiconductor Device Physics* (Academic, New York, 1992).
[21] T. Gonzalez and D. Pardo, J. Appl. Phys. **73**, 7453 (1993).
[22] A. Van der Ziel, *Noise in Solid State Devices and Circuits* (Wiley, New York, 1986).